Hindawi
Mathematical Problems in Engineering
Volume 2021, Article ID 5599624, 18 pages
https://doi.org/10.1155/2021/5599624

Research Article

An Optimal Design Method for Compliant Mechanisms

Ngoc Le Chau,[1] Ngoc Thoai Tran,[1] and Thanh-Phong Dao [2,3]

[1]*Faculty of Mechanical Engineering, Industrial University of Ho Chi Minh City, Ho Chi Minh City, Vietnam*
[2]*Division of Computational Mechatronics, Institute for Computational Science, Ton Duc Thang University, Ho Chi Minh City, Vietnam*
[3]*Faculty of Electrical & Electronics Engineering, Ton Duc Thang University, Ho Chi Minh City, Vietnam*

Correspondence should be addressed to Thanh-Phong Dao; daothanhphong@tdtu.edu.vn

Received 24 January 2021; Revised 10 February 2021; Accepted 18 February 2021; Published 2 March 2021

Academic Editor: Dr. Dilbag Singh

Compliant mechanisms are crucial parts in precise engineering but modeling techniques are restricted by a high complexity of their mechanical behaviors. Therefore, this paper devotes an optimal design method for compliant mechanisms. The integration method is a hybridization of statistics, finite element method, artificial intelligence, and metaheuristics. In order to demonstrate the superiority of the method, one degree of freedom is considered as a study object. Firstly, numerical datasets are achieved by the finite element method. Subsequently, the main design parameters of the mechanism are identified via analysis of variance. Desirability of both displacement and frequency of the mechanism is determined, and then, they are embedded inside a fuzzy logic system to combine into a single fitness function. Then, the relationship between the fine design variables and the fitness function is modeled using the adaptive network-based fuzzy inference system. Next, the single fitness function is maximized via moth-flame optimization algorithm. The optimal results determined that the frequency is 79.517 Hz and displacement is 1.897 mm. In terms of determining the global optimum solution, the current method is compared with the Taguchi, desirability, and Taguchi-integrated fuzzy methods. The results showed that the current method is better than those methods. Additionally, the devoted method outperforms the other metaheuristic algorithms such as TLBO, Jaya, PSOGSA, SCA, ALO, and LAPO in terms of faster convergence. The result of this study will be considered to apply for multiple-degrees-of-freedom compliant mechanisms in future work.

1. Introduction

Compliant mechanisms are specific mechanical devices, the mobility of which is inherently based on elastic energy [1–4]. Owing to the emerging strengths, compliant mechanisms have been receiving a great interest in industrial applications, for example, gripper [5], printing [6], nanopositioner [7], constant force mechanism [8], multistable equilibrium positions [9], micro-electromechanical systems [10], precision diamond turning [11], and energy harvesting [12]. Unlike rigid-body mechanisms, compliant mechanisms gain the excellent benefits such as a monolithic structure, lightweight, free friction, and free lubricant. On the other hand, rigid-body counterparts make friction and clearance thanks to kinematic joints such as revolute, prismatic, cylindrical, and spherical bearings or gears; meanwhile compliant mechanism gains smooth motions. By using rigid links and kinematic joints, rigid-body counterparts are easily analyzed through the traditional machines and mechanism theory [13]. On the contrary, theory for analyzing and synthesizing compliant mechanisms has been facing difficulties thanks to simultaneous coupling of kinematic and mechanical behaviors. Until now, a lot of different approaches for modeling compliant mechanism have been suggested, for example, pseudo-rigid-body model [14, 15], Castigliano [16], compliance [17], beam theory [18], dynamic stiffness [19], empirical technique [20], constraint-beam model [21], Euler-Bernoulli [22], and finite element method (FEM) [23]. In comparison with the mentioned methods, FEM is a useful tool for solving highly nonlinear problems.

To fulfill the gap between previous studies and the present study, an optimal design method is suggested. One-degree-of-freedom (DOF) compliant mechanism is employed as a study example to demonstrate the method's effectiveness. Regarding a fast tool servo [11], the 1-DOF requires a large range of displacement and a highly natural frequency. Besides, a small parasitic motion and stress are considered as two important constraints. Nowadays, optimization problem for compliant mechanisms can be classified into three main areas: topology optimization [24, 25], shape optimization, and size optimization [22, 26, 27]. In the present article, a multiobjective optimization (MOO) for the 1-DOF mechanism is proposed to improve its responses. Previously, there have been a few studies to deal with the MOO for compliant mechanisms but efficiency of techniques is still a challenge [28–30].

Moreover, there have been different types of optimization methods to deal with an optimization process. In general, a mathematical model is created before implementing a MOO problem. However, the analytical approaches have not been suitable for complex structures. In such a circumstance, data-based approaches are promising tools, which can predict and optimize the performances simultaneously. In order to save manufacturing costs, this article proposes a combination of numerical simulation, statistical techniques, and metaheuristics in terms of a reliable and global solution. Several approaches can be summarized as Taguchi [31], desirability [32], grey relation [33], and Taguchi-fuzzy (TF) [34] but most of them may reach a local solution. On the contrary, in order to achieve a global value, surrogate model is coupled with metaheuristics. The surrogate models include response surface approach [35, 36], Kriging [37], neural network [38], fuzzy [39], and adaptive-network-based fuzzy inference system [40]. Among them, adaptive-network-based fuzzy inference system (ANFIS) is an exact predictor. Related to metaheuristics, a variety of different algorithms were proposed, such as genetic algorithm [41], particle swarm optimization [42], and cuckoo search [43]. These metaheuristics require tuned parameters, such as teaching-learning-based algorithm [44], Jaya algorithm [45], and lightning attachment procedure optimization [46]. However, these algorithms are still limited by a low convergence speed. Then, other metaheuristics have been proposed to speed up the convergent time, for example, moth-flame optimization [47], ant lion optimizer [48], particle swarm optimization-based gravitational search algorithm [49], and sine-cosine algorithm [50]. In the present article, the moth-flame optimization is chosen for the 1-DOF mechanism due to its fast convergence.

The present paper aims to contribute an optimal design method for compliant mechanisms. The method undergoes six phases: Firstly, the nonlinear FEM is utilized to analyze the aforementioned behaviors of the 1-DOF mechanism. Secondly, some new populations for moth-flame optimization are discovered by investigating the sensitivity of parameters. Thirdly, real values of objective functions are converted into the desirability to suppress influences of units. Subsequently, fuzzy logic system is developed to bring all desirabilities into a single fitness function. The fitness function is defined as a combined objective function of multiple performances of the 1-DOF mechanism. Then, the relationship among the fine geometrical parameters and the established single fitness function is formulated through ANFIS model. Lastly, the single fitness function is then maximized via the moth-flame optimization. The remainder of this paper is organized as follows: Section 2 presents the computational method. A mechanical design of the 1-DOF mechanism is provided in Section 3. Practical implications and discussion are analyzed in Section 4. Conclusions are given in Section 5.

2. Optimal Design Method

In order to resolve a MOO for a 1-DOF mechanism, an optimal design framework is given (see in Figure 1). The optimization procedure is summarized by the following stages.

2.1. Stage 1: Initial Design. In the first stage, a draft model of the one-DOF mechanism is created. In this study, the computational method is offered to resolve MOO design for the 1-DOF mechanism. Numerical examples are investigated involving the usefulness of the developed computational method. The optimization process undergoes the following stepwise procedure.

Design Description. The 1-DOF compliant mechanism should achieve whole good frequency and displacement. Additionally, a small stress and parasitic motion are two constraints. In other words, a frequency aims to increase the response of system. A large displacement is expected to enlarge the range of positioning.

Design Variables. Geometrical parameters are identified as main design variables for 1-DOF compliant mechanism.

Objective Functions. Two design objectives include the frequency and the displacement.

3D Model. A 3D model is initialized, and then the frequency, displacement, parasitic motion, and stress are retrieved by finite element analysis (FEA) simulations.

Numerically Experimental Design. Numerical experiments are laid out by Box-Behnken design (BBD).

Numerical Dataset. Numerical datasets are retrieved through simulations.

Investigation of Sensitivity. Sensitivity analysis of all design variables is to identify several key parameters directly affecting both objective functions. On the other hand, this step determines design variables again and eliminates some low-significance parameters through analysis of variance (ANOVA).

Refined Design Variables. Main design variables are determined again to prepare several new population spaces for moth-flame optimization algorithm.

Redesigned Numerical Experiments. Numerical experiments are built again based on the refined design variables.

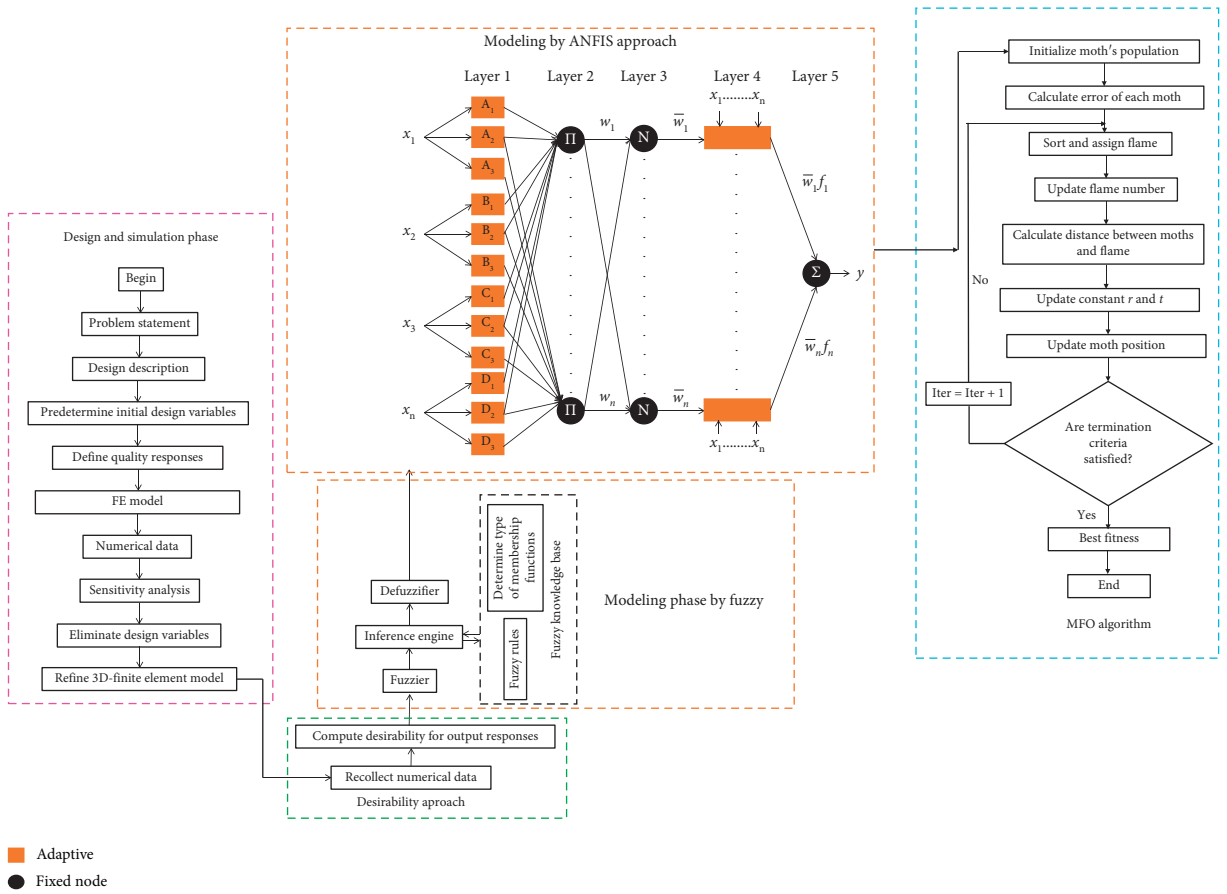

Figure 1: Flowchart of the optimal design method for compliant mechanisms.

Update 3D Model. 3D model is updated corresponding to a new population. Subsequently, numerical data are retrieved through FEA simulations.

2.2. Stage 2: Computation of Desirability Value. The aim of calculating the desirability is to suppress influences of different units among the frequency (Hz) and the displacement (mm). This stage undergoes some substeps as below.

Update Numerical Data. Numerical data are retrieved again based on the refined design variables.

Desirability Value. The desirability was utilized as a predictor. In this paper, the exponential type is used. The larger-the-better type is used for both objective functions in this article.

The larger-the-better type is explained as

$$\begin{cases} D_i = 0, & F^* \le B_L, \\ D_i = \left(\dfrac{F^* - B_L}{B_U - B_L}\right)^r, & B_L \le F^* \le B_U, \\ D_i = 1, & F^* \ge B_U, \end{cases} \tag{1}$$

where the desirability is denoted by Di. The ith objective function is denoted by F^*. B_L and B_U are lower range and upper range of F^*, respectively. R is desirability function index.

2.3. Stage 3: Modeling by the Fuzzy Logic System. The fuzzy logic system [51, 52] is employed to change both desirabilities into a single fitness function. Then, fuzzy inference system (FIS) is then utilized to generate a multiperformance characteristic index (MPCI) or the so-called single fitness function. This system is illustrated as shown in Figure 1.

2.4. Stage 4: Modeling by ANFIS. ANFIS is a popular technique by combining ANN and FIS [53]. The purpose of ANFIS model is to model the relations among the refined design variables and objective functions (see Figure 1). In this paper, datasets are divided into 70% for training and 30% for testing. Performances indexes, root mean square error (RMSE), and correlation coefficient (R^2) are utilized to evaluate the predictor.

2.5. Stage 5: Optimization Algorithm. Moth-flame algorithm (MFO) is mimicked by moth's behavior [47]. As moths see the light source, they fly in a spiral path. MFO has been successfully applied for many engineering areas thanks to simple usage and fast convergence rate. In this paper, MFO is extended to reach a global optimal design for the 1-DOF

mechanism. A maximum termination criterion is chosen as 10^5 in this study. More details of the MFO can be found in literature [47]. A flowchart of MFO is shown in Figure 1.

3. Numerical Study

The proposed 1-DOF mechanism is a potential positioner for precision system. This mechanism is expected to be used for a fast tool servo system whose applications can be found in the literatures [54–56]. In earlier design phase, in order to decrease the cost of a real fabrication process, the present study suggests a numerical optimization method for the 1-DOF mechanism.

3.1. Design Description. Figures 2(a) and 2(b) show 2D and 3D diagrams of 1-DOF compliant mechanism. In the middle, the mechanism is fixed holes. The mechanism includes three flexure hinges, named as FH-1, FH-2, and FH-3. Such FHs are connected through rigid links. The mechanism includes an input end (input load F of 25 N from an actuator) and an output is used to fix a cutting tool. The output displacement moves in vertical direction. At the same time, it also moves in horizontal direction, so-called parasitic motion. Flexure hinges with rectangular cross section permit a large displacement but this is a monolithic structure. Because it is subset of compliant mechanism and works in an elastic limitation of material, its motions are largely dependent on cross section of FHs; therefore, this article optimizes geometrical parameters of FHs. Some significant parameters of the proposed mechanism consist of dimensions of FHs [T_1, L_1, T_2, L_2, T_3, and L_3]. Remaining parameters (L, W, and H) are assigned as constant values. The 1-DOF mechanism is proposed for fast tool servo-assisted diamond cutting system to produce fined microstructure surfaces. Table 1 gives parameters of the mechanism. This mechanism is made by material Al 7075 with yield strength of 503 MPa.

3.2. Numerical Simulation. From Figure 2, a load of 25 N is employed to achieve the output response. Flexure hinges are refined two times to reach a good meshing. Solid 186 type of elements is used. The results determined that there are 747 elements and 5208 nodes, as depicted in Figure 3(a). In order to reach a better accuracy of simulation results, Skewness criteria are employed. The meshing result found that the value of this performance metric is about 0.40684, and this shows a good meshing quality (see Figure 3(b)).

3.3. Optimization Statement. As discussed above, the 1-DOF compliant mechanism is considered for translational manipulators where a high natural frequency over 70 Hz, a large displacement over 1.7 mm, a minimal parasitic motion under 0.02 mm, and a good strength are required. The optimization statement is described.

Find $\boldsymbol{x} = [T_1, L_1, T_2, L_2, T_3, L_3]^{\mathrm{T}}$.

$$\text{Maximize } f_1(x), \tag{2}$$

$$\text{Maximixe } f_2(x). \tag{3}$$

They are subject to constraints:

$$\begin{cases} f_1(x) \geq 70\,\text{Hz}, \\ f_2(x) \geq 1.7\,\text{mm}, \\ f_3(x) \leq 0.02\,\text{mm}, \\ f_4(x) \leq \dfrac{503\text{MPa}}{n}. \end{cases} \tag{4}$$

Initial space of design variables (unit: mm) is

$$\begin{cases} 0.72 \leq T_1 \leq 1.04, \\ 14.5 \leq L_1 \leq 16.5, \\ 0.45 \leq T_2 \leq 0.65, \\ 22.5 \leq L_2 \leq 27.5, \\ 0.54 \leq T_3 \leq 0.78, \\ 18 \leq L_3 \leq 22. \end{cases} \tag{5}$$

$f_1(\boldsymbol{x})$, $f_2(\boldsymbol{x})$, $f_3(\boldsymbol{x})$, and $f_4(\boldsymbol{x})$ represent natural frequency, displacement, parasitic error, and stress correspondingly. N is safety factor. The ranges of parameters are determined based on the experiences in the field and further fabrication capacity of devices.

4. Practical Implications and Discussion

4.1. Determination of Main Parameters. Involving whole initial design variables, design of numerical experiments is built by BBD technique. Table 2 gives initial design parameters and their ranges. Each experiment is implemented by simulations. The initial results are retrieved in Table 3.

Case study 1 focuses on the sensitivity analysis for the natural frequency. In Table 4, the results of ANOVA determined that T_1 with contribution of 0.02% and L_1 with contribution of 0% and their p values are 0.567 and 0.891, which are larger than 0.05. The contributions of T_1 and L_1 are very small, and they are therefore deleted from modeling and optimization process. Additionally, a matrix plot is drawn to show effects of all parameters on the frequency. As seen in Figure 4, it also has a similar conclusion in Table 4. To summarize, case study 1 deals with the main design parameters, including T_2, L_2, T_3, and L_3.

Case study 2 deals with the sensitivity analysis for displacement. Based on the ANOVA results in Table 5, the parameter's contributions T_1, L_1, and L_3 are very small with 1.57%, 1.33%, and 1.86%, respectively.

The results of Figure 5 also have the same conclusion in Table 5. It means that the parameters T_1, L_1, and L_3 should be suppressed during modeling and optimization procedure.

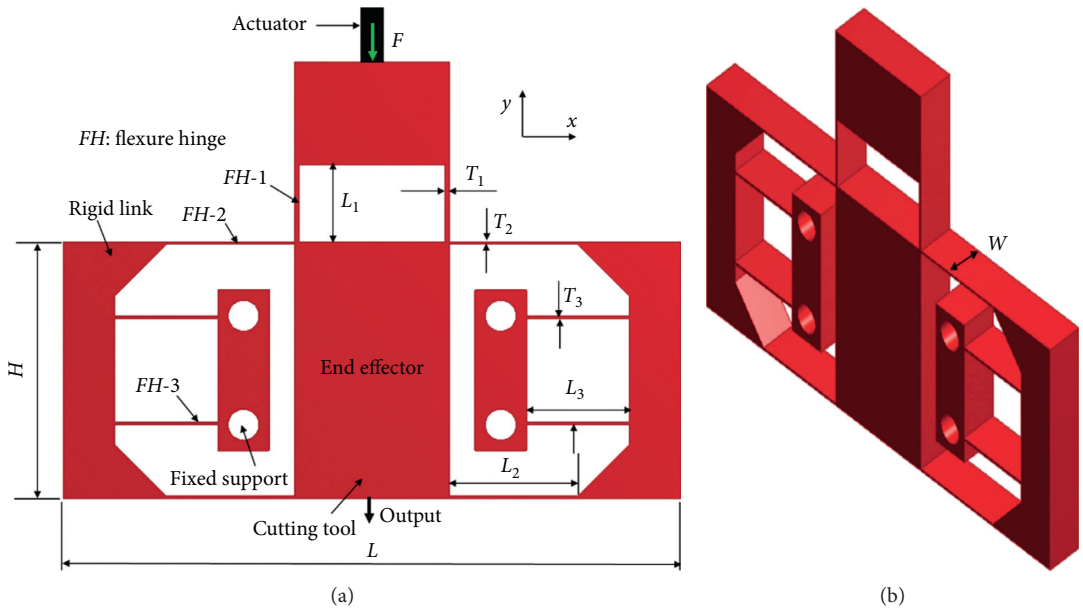

Figure 2: (a) 2D diagram and (b) 3D model (unit: mm).

Table 1: Parameters.

Symbol	Value
T_1	$0.72\text{ mm} \le T_1 \le 1.04\text{ mm}$
L_1	$14.5\text{ mm} \le L_1 \le 16.5\text{ mm}$
T_2	$0.45\text{ mm} \le T_2 \le 0.65\text{ mm}$
L_2	$22.5 \le L_2 \le 27.5$
T_3	$0.54\text{ mm} \le T_3 \le 0.78\text{ mm}$
L_3	$18\text{ mm} \le L_3 \le 22\text{ mm}$
W	10 mm
H	50 mm
L	120 mm

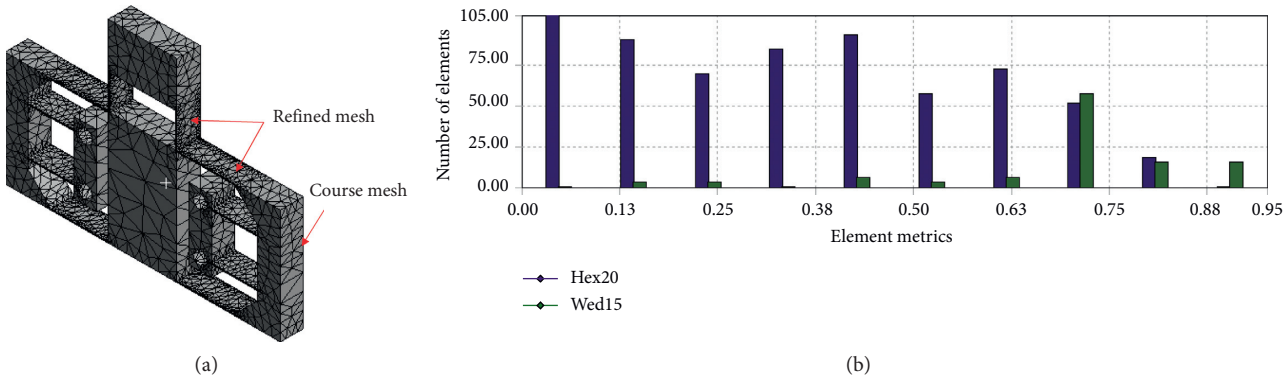

Figure 3: Simulation setup: (a) meshing process; (b) metric distribution of mesh.

4.2. Modeling and Optimization

4.2.1. Determination of MFs Types. Table 6 assigns the fuzzy variables for MFs. In this article, the frequency and displacement desirabilities are two inputs of the FIS. The MFs types for two inputs and an output of the FIS system are illustrated in Figures 6 and 7.

4.2.2. Investigation on Case Study 1. As discussed in the previous section, overall initial design variables are limited. Those factors actually contribute the responses of 1-DOF mechanism. Besides, spaces of parameters are newly initialized for the modeling and optimization process. The optimization formulation is stated as follows.

Find $\boldsymbol{x} = [T_2, L_2, T_3, L_3]^{\mathrm{T}}$.

Table 2: Initial design variables and range (unit: mm).

Notation	Range	Level 1	Level 2	Level 3
T_1	$0.72 \le T_1 \le 1.04$	0.72	0.88	1.04
L_1	$14.5 \le L_1 \le 16.5$	14.5	15.5	16.5
T_2	$0.45 \le T_2 \le 0.65$	0.45	0.55	0.65
L_2	$22.5 \le L_2 \le 27.5$	22.5	24.5	27.5
T_3	$0.54 \le T_3 \le 0.78$	0.54	0.66	0.78
L_3	$18 \le L_3 \le 22$	18	20	22

Table 3: Initial results.

Trial	Parameters (unit: mm)						Frequency (Hz)	Displacement (mm)	Parasitic motion (mm)	Stress (MPa)
	$T1$	$L1$	$T2$	$L2$	$T3$	$L3$	$f_1(x)$	$f_2(x)$	$f_3(x)$	$f_4(x)$
1	0.88	15	0.55	25	0.66	20	103.9916	0.9335	0.0124	162.70
2	0.72	13.5	0.55	22.5	0.66	20	112.9361	0.7761	0.0110	131.69
3	1.04	13.5	0.55	22.5	0.66	20	112.5340	0.7787	0.0112	134.38
4	0.72	16.5	0.55	22.5	0.66	20	113.4298	0.7663	0.0106	130.98
5	1.04	16.5	0.55	22.5	0.66	20	112.3602	0.7783	0.0111	134.12
6	0.72	13.5	0.55	27.5	0.66	20	91.0306	1.2335	0.0158	151.30
7	1.04	13.5	0.55	27.5	0.66	20	90.5761	1.2475	0.0165	167.17
8	0.72	16.5	0.55	27.5	0.66	20	92.1246	1.2013	0.0157	159.17
9	1.04	16.5	0.55	27.5	0.66	20	91.8895	1.1985	0.0157	159.29
10	0.88	13.5	0.45	25	0.54	20	87.7464	1.2845	0.0130	152.76
11	0.88	16.5	0.45	25	0.54	20	85.4190	1.3601	0.0139	151.35
12	0.88	13.5	0.65	25	0.54	20	101.8192	0.8786	0.0102	108.25
13	0.88	16.5	0.65	25	0.54	20	101.1571	0.8922	0.0103	106.90
14	0.88	13.5	0.45	25	0.78	20	102.5691	0.9977	0.0128	151.42
15	0.88	16.5	0.45	25	0.78	20	100.4735	1.0362	0.0130	154.94
16	0.88	13.5	0.65	25	0.78	20	127.6535	0.6216	0.0104	107.23
17	0.88	16.5	0.65	25	0.78	20	129.2442	0.6042	0.0101	106.92
18	0.88	15	0.45	22.5	0.66	18	103.2041	0.9834	0.0155	152.76
19	0.88	15	0.65	22.5	0.66	18	136.8287	0.5197	0.0082	93.28
20	0.88	15	0.45	27.5	0.66	18	76.0515	1.7637	0.0210	225.27
21	0.88	15	0.65	27.5	0.66	18	112.5988	0.7996	0.0117	109.54
22	0.88	15	0.45	22.5	0.66	22	94.8556	1.1217	0.0155	152.93
23	0.88	15	0.65	22.5	0.66	22	117.4083	0.6527	0.0080	87.21
24	0.88	15	0.45	27.5	0.66	22	72.7104	1.9120	0.0210	227.36
25	0.88	15	0.65	27.5	0.66	22	102.5106	0.9322	0.0119	109.20
26	0.72	15	0.55	22.5	0.54	20	98.0539	0.9619	0.0110	130.67
27	1.04	15	0.55	22.5	0.54	20	98.0751	0.9551	0.0109	132.22
28	0.72	15	0.55	27.5	0.54	20	85.1501	1.3671	0.0153	157.48
29	1.04	15	0.55	27.5	0.54	20	85.2019	1.3584	0.0156	157.87
30	0.72	15	0.55	22.5	0.78	20	123.7692	0.6668	0.0106	134.85
31	1.04	15	0.55	22.5	0.78	20	122.5388	0.6766	0.0106	136.39
32	0.72	15	0.55	27.5	0.78	20	96.0811	1.1188	0.0157	160.43
33	1.04	15	0.55	27.5	0.78	20	94.7834	1.1495	0.0161	170.74
34	0.88	13.5	0.55	25	0.54	18	98.0678	1.0340	0.0130	168.07
35	0.88	16.5	0.55	25	0.54	18	97.2716	1.0484	0.0128	155.91
36	0.88	13.5	0.55	25	0.78	18	112.3299	0.8237	0.0129	166.04
37	0.88	16.5	0.55	25	0.78	18	103.9916	0.8218	0.0127	164.79
38	0.88	13.5	0.55	25	0.54	22	112.9361	1.2757	0.0127	165.29
39	0.88	16.5	0.55	25	0.54	22	112.5340	1.2779	0.0139	150.35
40	0.88	13.5	0.55	25	0.78	22	113.4298	0.9178	0.0135	159.05
41	0.88	16.5	0.55	25	0.78	22	112.3602	0.9198	0.0130	166.97
42	0.72	15	0.45	25	0.66	18	91.0306	1.0412	0.0130	152.59
43	1.04	15	0.45	25	0.66	18	90.5761	1.0872	0.0133	149.97
44	0.72	15	0.65	25	0.66	18	92.1246	0.6397	0.0102	106.64
45	1.04	15	0.65	25	0.66	18	91.8895	0.6404	0.0102	106.75
46	0.72	15	0.45	25	0.66	22	87.7464	1.2074	0.0135	155.46
47	1.04	15	0.45	25	0.66	22	85.4190	1.2152	0.0134	151.53
48	0.72	15	0.65	25	0.66	22	101.8192	0.7750	0.0102	107.25
49	1.04	15	0.65	25	0.66	22	111.3604	0.7615	0.0100	106.38

Table 4: The frequency's ANOVA.

Source	Df	Seq SS	Contribution	Adj SS	Adj MS	F value	p value
Model	27	9662.88	98.63	9662.88	357.88	55.89	≤0.001
Linear	6	9110.08	92.99	9110.08	1518.35	237.10	≤0.001
T_1	1	2.16	0.02	2.16	2.16	0.34	0.567
L_1	1	0.12	0.00	0.12	0.12	0.02	0.891
T_2	1	3680.14	37.56	3680.14	3680.14	574.67	≤0.001
L_2	1	2715.44	27.72	2715.44	2715.44	424.03	≤0.001
T_3	1	2085.91	21.29	2085.91	2085.91	325.72	≤0.001
L_3	1	626.31	6.39	626.31	626.31	97.80	≤0.001
Square	6	250.43	2.56	250.43	41.74	6.52	0.001
$T_1 * T_1$	1	7.11	0.07	12.26	12.26	1.91	0.181
$L_1 * L_1$	1	4.49	0.05	0.40	0.40	0.06	0.804
$T_2 * T_2$	1	186.44	1.90	39.17	39.17	6.12	0.022
$L_2 * L_2$	1	30.95	0.32	51.60	51.60	8.06	0.010
$T_3 * T_3$	1	8.50	0.09	19.64	19.64	3.07	0.095
$L_3 * L_3$	1	12.95	0.13	12.95	12.95	2.02	0.170
2-Way interaction	15	302.36	3.09	302.36	20.16	3.15	0.008
$T_1 * L_1$	1	0.03	0.00	0.03	0.03	0.00	0.951
$T_1 * T_2$	1	1.29	0.01	1.29	1.29	0.20	0.658
$T_1 * L_2$	1	0.03	0.00	0.03	0.03	0.01	0.942
$T_1 * T_3$	1	0.85	0.01	0.85	0.85	0.13	0.720
$T_1 * L_3$	1	1.07	0.01	1.07	1.07	0.17	0.687
$L_1 * T_2$	1	3.58	0.04	3.58	3.58	0.56	0.463
$L_1 * L_2$	1	0.54	0.01	0.54	0.54	0.09	0.773
$L_1 * T_3$	1	0.65	0.01	0.65	0.65	0.10	0.754
$L_1 * L_3$	1	0.03	0.00	0.03	0.03	0.00	0.950
$T_2 * L_2$	1	12.93	0.13	12.93	12.93	2.02	0.170
$T_2 * T_3$	1	72.27	0.74	72.27	72.27	11.28	0.003
$T_2 * L_3$	1	59.82	0.61	59.82	59.82	9.34	0.006
$L_2 * T_3$	1	110.01	1.12	110.01	110.01	17.18	≤0.001
$L_2 * L_3$	1	25.70	0.26	25.70	25.70	4.01	0.058
$T_3 * L_3$	1	13.58	0.14	13.58	13.58	2.12	0.160
Error	21	134.48	1.37	134.48	6.40		
Total	48	9797.36	100.00				

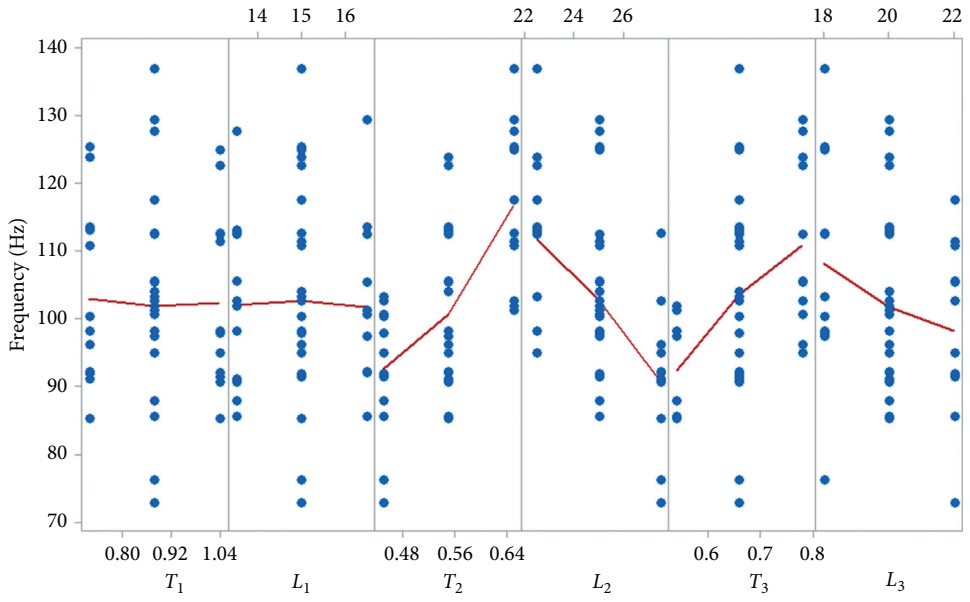

Figure 4: Sensitivity plot of the frequency.

Table 5: The displacement's ANOVA.

Source	Df	Seq SS	Contribution (%)	Adj SS	Adj MS	F value	p value
Model	27	5.82988	83.26	5.82988	0.21592	3.87	0.001
Linear	6	4.59442	65.61	4.59442	0.76574	13.72	≤0.001
T_1	1	0.10993	1.57	0.10993	0.10993	1.97	0.175
L_1	1	0.09339	1.33	0.09339	0.09339	1.67	0.210
T_2	1	1.64995	23.56	1.64995	1.64995	29.56	≤0.001
L_2	1	2.14644	30.65	2.14644	2.14644	38.45	≤0.001
T_3	1	0.46472	6.64	0.46472	0.46472	8.33	0.009
L_3	1	0.12999	1.86	0.12999	0.12999	2.33	0.142
Square	6	0.39032	5.57	0.39032	0.06505	1.17	0.361
$T_1 * T_1$	1	0.11508	1.64	0.04557	0.04557	0.82	0.376
$L_1 * L_1$	1	0.17138	2.45	0.05944	0.05944	1.06	0.314
$T_2 * T_2$	1	0.02833	0.40	0.00082	0.00082	0.01	0.905
$L_2 * L_2$	1	0.00016	0.00	0.02704	0.02704	0.48	0.494
$T_3 * T_3$	1	0.05103	0.73	0.07537	0.07537	1.35	0.258
$L_3 * L_3$	1	0.02435	0.35	0.02435	0.02435	0.44	0.516
2-Way interaction	15	0.84514	12.07	0.84514	0.05634	1.01	0.482
$T_1 * L_1$	1	0.29077	4.15	0.29077	0.29077	5.21	0.033
$T_1 * T_2$	1	0.00055	0.01	0.00055	0.00055	0.01	0.922
$T_1 * L_2$	1	0.14384	2.05	0.14384	0.14384	2.58	0.123
$T_1 * T_3$	1	0.00039	0.01	0.00039	0.00039	0.01	0.934
$T_1 * L_3$	1	0.00034	0.00	0.00034	0.00034	0.01	0.938
$L_1 * T_2$	1	0.00173	0.02	0.00173	0.00173	0.03	0.862
$L_1 * L_2$	1	0.26707	3.81	0.26707	0.26707	4.78	0.040
$L_1 * T_3$	1	0.00045	0.01	0.00045	0.00045	0.01	0.929
$L_1 * L_3$	1	0.00001	0.00	0.00001	0.00001	0.00	0.990
$T_2 * L_2$	1	0.12778	1.82	0.12778	0.12778	2.29	0.145
$T_2 * T_3$	1	0.00054	0.01	0.00054	0.00054	0.01	0.923
$T_2 * L_3$	1	0.00022	0.00	0.00022	0.00022	0.00	0.951
$L_2 * T_3$	1	0.00170	0.02	0.00170	0.00170	0.03	0.863
$L_2 * L_3$	1	0.00001	0.00	0.00001	0.00001	0.00	0.989
$T_3 * L_3$	1	0.00974	0.14	0.00974	0.00974	0.17	0.680
Error	21	1.17221	16.74	1.17221	0.05582		
Total	48	7.00209	100.00				

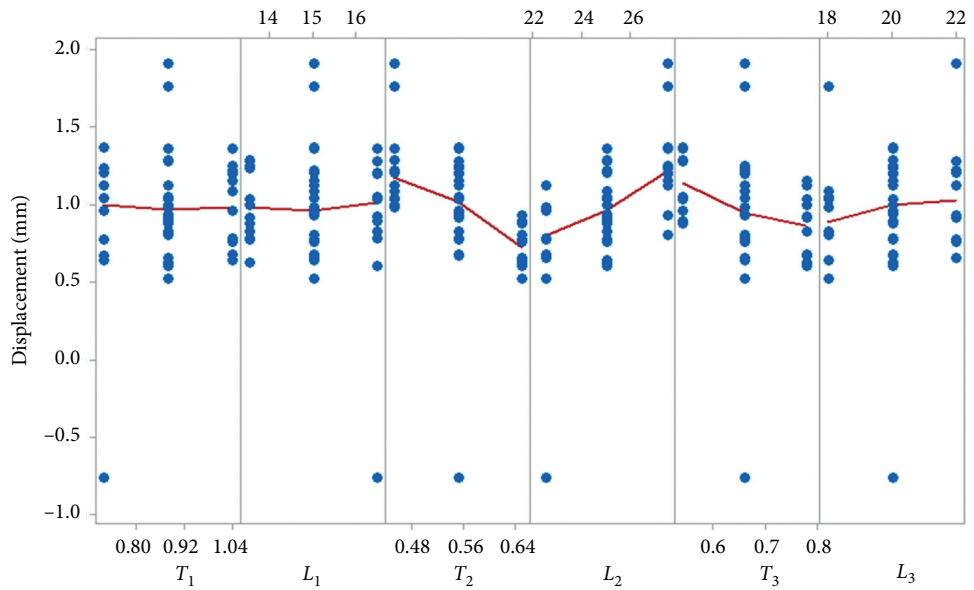

Figure 5: Sensitivity plot of the displacement.

Table 6: Proposed fuzzy variables.

Abbreviation	SS	RS	S	SA	A	AL	NL	L	SL
Fuzzy variable	So small	Relatively small	Small	Small average	Average	Average large	Near large	Large	So large

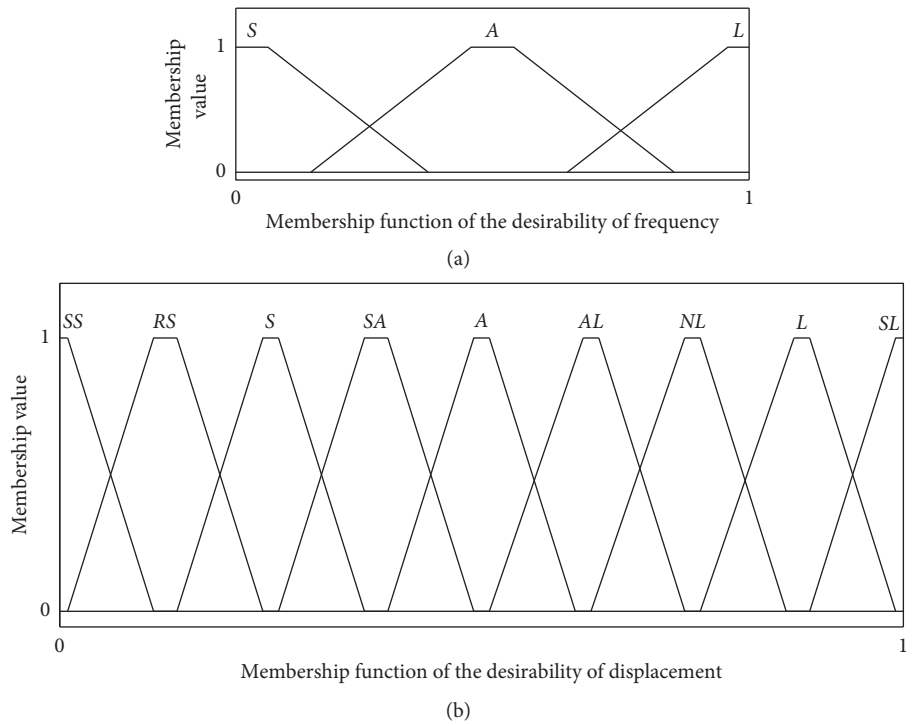

Figure 6: MFs types: (a) the frequency and (b) the displacement.

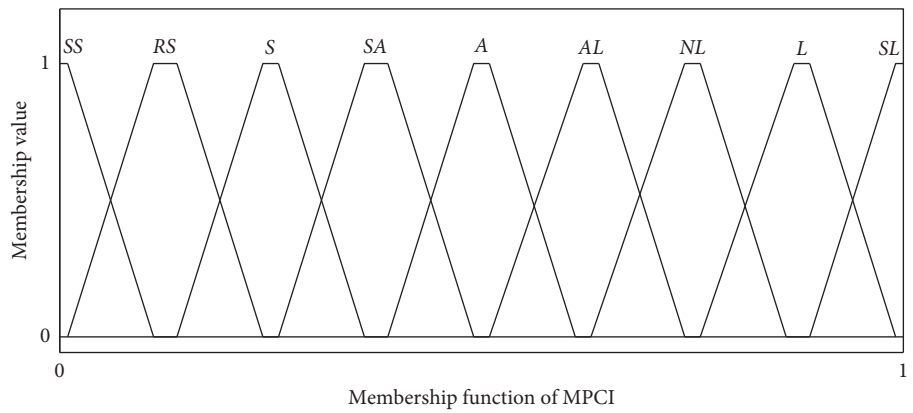

Figure 7: MFs type for the output of FIS system.

$$\text{Maximize } f(x)_{\text{case1}}, \tag{6}$$

$$s.t. \begin{cases} f_1(x) \geq 70\text{Hz}, \\ f_2(x) \geq 1.7\text{mm}, \\ f_3(x) \leq 0.02\text{mm}, \\ f_4(x) \leq \dfrac{503\text{MPa}}{n}, \\ 0.45\text{mm} \leq T_2 \leq 0.65\text{mm}, \\ 22.5\text{mm} \leq L_2 \leq 27.5\text{mm}, \\ 0.54\text{mm} \leq T_3 \leq 0.78\text{mm}, \\ 18\text{mm} \leq L_3 \leq 22\text{mm}. \end{cases} \tag{7}$$

$f(\boldsymbol{x})$ is a single fitness function. Table 7 shows the results for case study 1. Table 8 presents the MFs variables for the fuzzy if-then rules in modeling both objective functions into a single objective function.

Relationship plot of the output versus inputs in the FIS modeling is illustrated in Figure 8. Figure 9 gives the fuzzy if-then rules.

Figure 9 illustrates the fuzzy rules. When D_1 value is input into the left column and D_2 value is input into the middle column, the output of FIS is found in the right column of Figure 9, respectively. Table 9 gives the results of the output of FIS.

Next, ANFIS modeling is built based on Tables 7 and 9 in MATLAB R2019b. In the developed model, there are nodes of 193, linear parameters of 405, nonlinear parameters of 36, total parameters of 441, training data of 17, testing data of 8,

Table 7: Case study 1: simulated results.

Trial	Refined parameters (unit: mm)				Frequency	Displacement	Parasitic motion	Stress
	T_2	L_2	T_3	L_3	$f_1(x)$ (Hz)	$f_2(x)$ (mm)	$f_3(x)$ (mm)	$f_4(x)$ (MPa)
1	0.55	25	0.66	20	104.0482	0.9336	0.0124	162.7355
2	0.45	22.5	0.66	20	99.3184	1.0459	0.0155	153.0472
3	0.65	22.5	0.66	20	127.1888	0.5806	0.0081	92.9516
4	0.45	27.5	0.66	20	74.1823	1.8419	0.0211	227.1803
5	0.65	27.5	0.66	20	107.0481	0.8742	0.0120	117.8249
6	0.55	25	0.54	18	98.7476	1.0189	0.0127	165.1369
7	0.55	25	0.78	18	112.5295	0.8221	0.0127	164.9785
8	0.55	25	0.54	22	85.9801	1.2611	0.0132	158.4125
9	0.55	25	0.78	22	105.5051	0.9183	0.0129	164.3392
10	0.45	25	0.66	18	100.1899	1.0411	0.0130	152.5881
11	0.65	25	0.66	18	124.0486	0.6519	0.0100	107.2939
12	0.45	25	0.66	22	91.6971	1.2088	0.0136	155.6330
13	0.65	25	0.66	22	111.4232	0.7671	0.0102	105.6065
14	0.55	22.5	0.54	20	98.0046	0.9620	0.0110	130.6791
15	0.55	27.5	0.54	20	85.3761	1.3584	0.0155	158.0305
16	0.55	22.5	0.78	20	123.7160	0.6666	0.0106	134.8080
17	0.55	27.5	0.78	20	96.1152	1.1131	0.0157	159.7465
18	0.45	25	0.54	20	88.2632	1.2665	0.0129	152.1337
19	0.65	25	0.54	20	101.8941	0.8819	0.0102	109.0929
20	0.45	25	0.78	20	102.2331	1.0051	0.0130	150.8916
21	0.65	25	0.78	20	128.5677	0.6122	0.0100	105.7656
22	0.55	22.5	0.66	18	121.7163	0.6803	0.0111	135.3569
23	0.55	27.5	0.66	18	94.8892	1.1449	0.0156	161.3298
24	0.55	22.5	0.66	22	106.9204	0.8358	0.0106	134.3837
25	0.55	27.5	0.66	22	87.8279	1.3095	0.0161	150.2442

Table 8: Proposed fuzzy if-then rules.

Trial	D_1 of $f_1(x)$	D_2 of $f_2(x)$	Output
1	*S*	*SS*	*SS*
2	*A*	*SS*	*RS*
3	*L*	*SS*	*S*
4	*S*	*RS*	*SS*
5	*A*	*RS*	*S*
6	*L*	*RS*	*SA*
7	*S*	*S*	*S*
8	*A*	*S*	*SA*
9	*L*	*S*	*AL*
10	*S*	*SA*	*S*
11	*A*	*SA*	*SA*
12	*L*	*SA*	*A*
13	*S*	*A*	*SA*
14	*A*	*A*	*A*
15	*L*	*A*	*AL*
16	*S*	*AL*	*SA*
17	*A*	*AL*	*A*
18	*L*	*AL*	*AL*
19	*S*	*NL*	*AL*
20	*A*	*NL*	*AL*
21	*L*	*NL*	*L*
22	*S*	*L*	*AL*
23	*A*	*L*	*L*
24	*L*	*L*	*NL*
25	*S*	*SL*	*AL*
26	*A*	*SL*	*L*
27	*L*	*SL*	*SL*

D_1 and D_2 are desirabilities of frequency and displacement, respectively

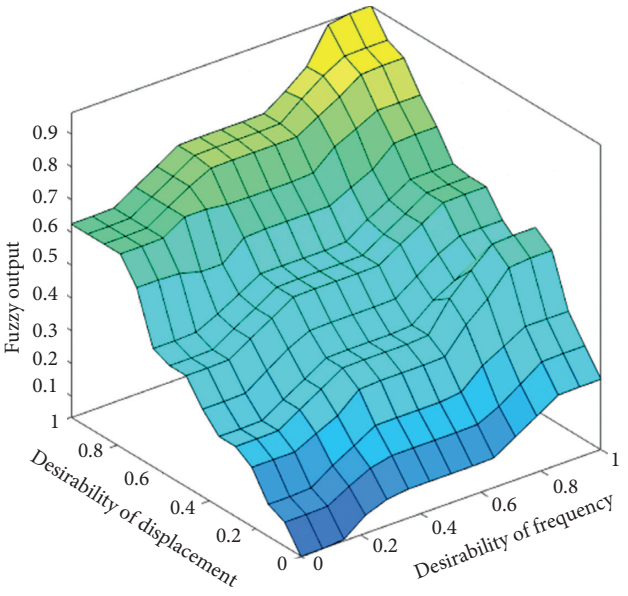

Figure 8: Relationship plot in the FIS modeling.

and fuzzy if-then rules of 81. The built ANFIS model has relatively good performance indexes with R^2 of 0.963 and RMSE of 0.035.

In this study, two objective functions are combined into a single objective function by using the FIS. The output of the FIS is the single objective function, which can be optimized by many methods. Then, the displacement and frequency

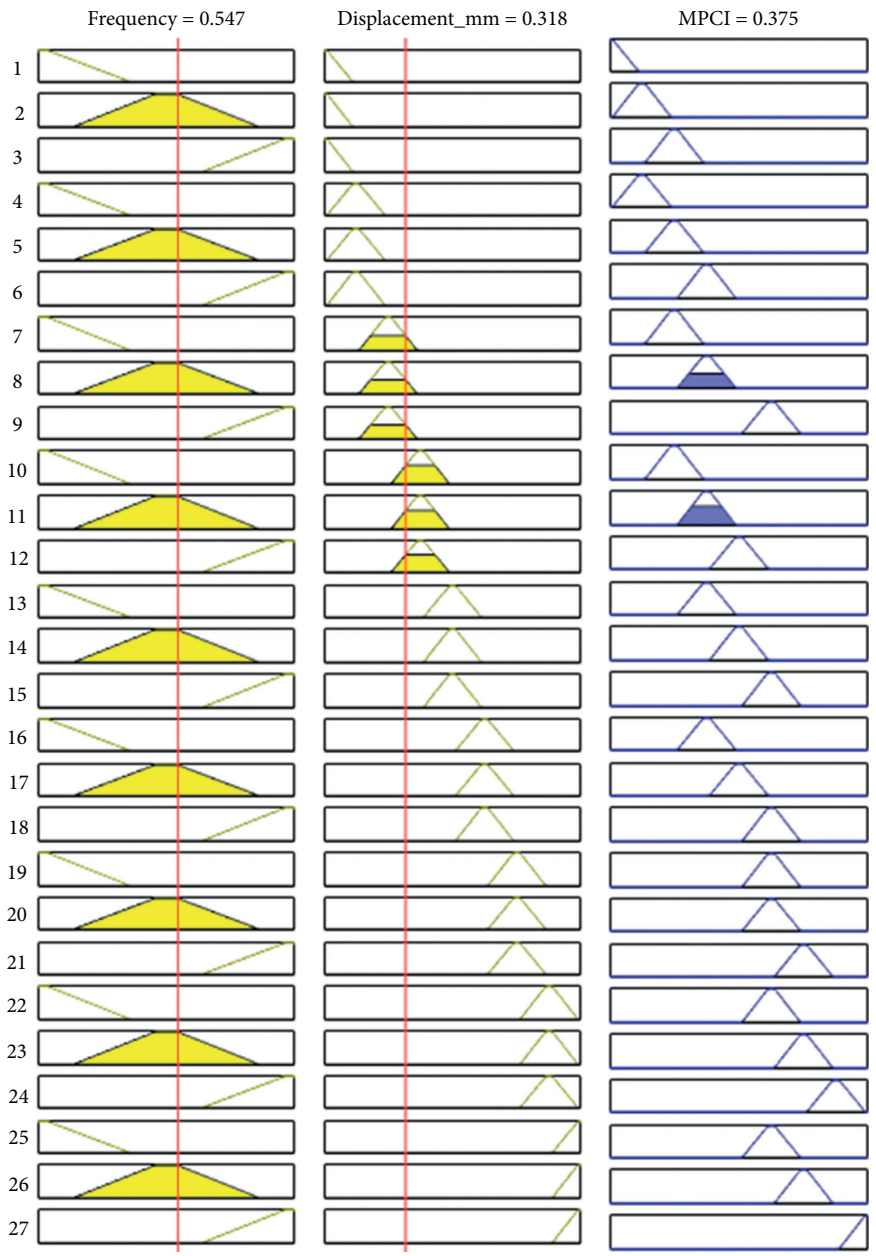

Figure 9: Illustration of the fuzzy if-then rules in the FIS modeling.

Table 9: Case study 1: output of FIS.

Trial	D_1 of f_1 (x)	D_2 of f_2 (x)	Output
1	0.549153709	0.279844008	0.375
2	0.545631181	0.271824854	0.375
3	0.94187745	0.069056252	0.319
4	0.096943974	0.850288316	0.625
5	0.585043702	0.249264885	0.375
6	0.472916027	0.311560512	0.375
7	0.758444845	0.156517523	0.398
8	0.227762156	0.493821918	0.425
9	0.618891448	0.223017636	0.352
10	0.442532311	0.413803418	0.412
11	0.922698148	0.032683298	0.279
12	0.288171515	0.558960074	0.459

Table 9: Continued.

Trial	D_1 of $f_1(x)$	D_2 of $f_2(x)$	Output
13	0.692351675	0.13628816	0.281
14	0.438830692	0.297635129	0.375
15	0.17371882	0.657096979	0.45
16	0.914808353	0.064837296	0.315
17	0.37439927	0.46404754	0.466
18	0.221158841	0.613630915	0.422
19	0.546539128	0.215051828	0.343
20	0.442695186	0.404024209	0.4
21	1	0	0.25
22	0.841975976	0.098401988	0.335
23	0.368106025	0.474134093	0.478
24	0.578512868	0.219178805	0.348
25	0.246861864	0.602118795	0.436

can be predicted based on the optimal design variables. Specifically, Taguchi can optimize the single fitness function but may trap a local optimum value; meanwhile MFO algorithm can search a global optimum value. Hence, the optimal values from the Taguchi are compared with those found by the proposed method's framework. The purpose of this comparison is to clearly demonstrate the usefulness of the devoted method in searching the global solution.

In Table 10, the optimal parameters by the TF include $T_2 = 0.45$ mm, $L_2 = 27.5$ mm, $T_3 = 0.54$ mm, and $L_3 = 20$ mm. The results of TF show the frequency, displacement, parasitic error, and stress are approximately 75.871 Hz and 1.776 mm, 0.019 mm, and 212.114 MPa, respectively. However, those optimal values can trap local optimum solutions. To find a global optimum solution, moth-flame optimization algorithm is adopted. The results of the hybrid computational method determine $T_2 = 0.45$ mm, $L_2 = 27.5$ mm, $T_3 = 0.78$ mm, and $L_3 = 18$ mm (Table 10). The frequency, displacement, parasitic error, and stress are about 85.174 Hz and 2.447 mm, 0.016 mm, and 145.982 MPa, respectively. Furthermore, the MPCI in the hybrid computational method is better than that in TF. It means that the hybrid computational method outperformed the TF.

4.2.3. Investigation on Case Study 2. Initialized from Table 5 and Figure 7, the space of design parameters is also limited to generate a new population for the modeling and optimization procedure. The optimization formulation is stated as follows.

Search $\boldsymbol{x} = [T_2, L_2, T_3,]^{\mathrm{T}}$.

$$\text{Maximize } f(x)_{\text{case 2}}, \tag{8}$$

$$s.t. \begin{cases} f_1(x) \geq 1.7 \text{ Hz}, \\ f_2(x) \geq 1.7 \text{ mm}, \\ f_3(x) \leq 0.02 \text{ mm}, \\ f_4(x) \leq \dfrac{503\text{MPa}}{n}, \\ 0.45 \text{ mm} \leq T_2 \leq 0.65 \text{ mm}, \\ 22.5 \text{ mm} \leq L_2 \leq 27.5 \text{ mm}, \\ 0.54 \text{ mm} \leq T_3 \leq 0.78 \text{ mm}. \end{cases} \tag{9}$$

Table 11 gives the results of 13 numerical experiments, including the frequency, the displacement, the parasitic motion, and stress. The desirabilities are calculated (Table 12).

Subsequently, the fuzzy if-then rules are built based on Table 8, and the output of FIS system is given in Table 12.

In this ANFIS model, there are nodes of 34, linear parameters of 32, nonlinear parameters of 18, total parameters of 50, training data of 9, testing data of 4, and fuzzy if-then rules of 8. The developed ANFIS modeling achieves relatively good performance indexes with R^2 of 0.954 and RMSE of 0.012.

Using TF, the optimal parameters are $T_2 = 0.45$ mm, $L_2 = 27.5$ mm, and $T_3 = 0.66$ mm (Table 13). The frequency, displacement, parasitic error, and stress are about 79.460 Hz, 1.637 mm, 0.018 mm, and 198.015 MPa, respectively. The safety factor is determined to be about 2.54. The optimal solutions are local solutions.

In Table 13, using the hybrid computational method, the optimal parameters are $T_2 = 0.45$ mm, $L_2 = 27.5$ mm, and $T_3 = 0.69$ mm. The optimal frequency, displacement, parasitic error, equivalent stress, and safety factor are 76.743 Hz, 1.700 mm, 0.019 mm, 236.027 MPa, and 2.131, respectively. It is noted that the MPCI in the hybrid computational method is also better than that in the TF.

4.3. Discussion. In the previous sections, the sensitivity of factors on the output responses is analyzed to redetermine the main geometrical parameters. Those parameters contribute directly the frequency, displacement, parasitic motion, and stress of 1-DOF mechanism. Two numerical examples are studied. In order to calculate an error among the predicted value (R_p) and simulation (R_s), the error (E) is calculated as

$$E(\%) = \left(\frac{R_p - R_s}{R_s} - 1 \right) * 100. \tag{10}$$

A comparison with case 1 is performed. Using the computational method, the error is around 7% for case study 1 and 3.8% for case 2. On the contrary, using TF, the error is 23% for case 1 and 14.7% for case 2 (Table 14). Additionally, the computational methodology can reach a global solution.

Table 10: Case study 1: the optimal results.

Method	Optimal parameters	Optimal results					
		MPCI	$f_1(x)$ (HZ)	$f_2(x)$ (mm)	$f_3(x)$ (mm)	$f_4(x)$ (MPa)	n-safety factor
TF	$T_2 = 0.45$ $L_2 = 27.5$ $T_3 = 0.54$ $L_3 = 20$	0.628	75.8711	1.77636	0.0198	212.114	2.731
The current method	$T_2 = 0.45$ $L_2 = 27.5$ $T_3 = 07.8$ $L_3 = 18$	0.848	85.1749	2.4472	0.0160	145.982	3.468

Table 11: Case study 2: simulated results.

Trial	Refined variables (unit: mm)			Frequency	Displacement	Parasitic	Stress
	T_2	L_2	T_3	$f_1(x)$ (Hz)	$f_2(x)$ (mm)	$f_3(x)$ (mm)	$f_4(x)$ (MPa)
1	0.55	25	0.66	104.0482	0.9336	0.0124	162.7355
2	0.45	22.5	0.66	99.31841	1.0459	0.0155	153.0472
3	0.65	22.5	0.66	127.1888	0.5806	0.0081	92.95158
4	0.45	27.5	0.66	74.18228	1.8419	0.0211	227.1803
5	0.65	27.5	0.66	107.0481	0.8742	0.0120	117.8249
6	0.45	25	0.54	88.26316	1.2665	0.0129	152.1337
7	0.65	25	0.54	101.8941	0.8819	0.0102	109.0929
8	0.45	25	0.78	102.2331	1.0051	0.0130	150.8916
9	0.65	25	0.78	128.5677	0.6122	0.0100	105.7656
10	0.55	22.5	0.54	98.00464	0.9620	0.0110	130.6791
11	0.55	27.5	0.54	85.37607	1.3584	0.0155	158.0305
12	0.55	22.5	0.78	123.716	0.6666	0.0106	134.808
13	0.55	27.5	0.78	96.11523	1.1131	0.0157	159.7465

Table 12: Case study 2: results of the output of FIS system.

Trial	D_1 of $f_1(x)$	D_2 of $f_2(x)$	Output
1	0.549153709	0.279844008	0.375
2	0.498323931	0.328431242	0.375
3	0.915304881	0.089411622	0.342
4	0.059341072	0.910588378	0.625
5	0.56817548	0.273313929	0.375
6	0.220806827	0.60972779	0.421
7	0.566921796	0.174897685	0.299
8	0.458401921	0.400613918	0.395
9	1	0	0.25
10	0.439992178	0.276996376	0.375
11	0.184584653	0.640151901	0.409
12	0.932028588	0.044691377	0.294
13	0.401323853	0.447595295	0.448

Table 13: Case study 2: the optimal results.

Method	Optimal parameters (mm)	Optimal results					
		MPCI	Frequency $f_1(x)$ (HZ)	Displacement $f_2(x)$ (mm)	Parasitic $f_3(x)$ (mm)	Stress $f_4(x)$ (MPa)	n-safety factor
TF	$T_2 = 0.45$ $L_2 = 27.5$ $T_3 = 0.66$	0.5568	79.4601	1.6371	0.0184	198.015	2.540
Computational method	$T_2 = 0.45$ $L_2 = 27.5$ $T_3 = 0.69$	0.6402	76.7435	1.7002	0.0197	236.027	2.131

Table 14: Comparison results of two cases.

Case study		Parameters (mm)	Optimal responses					
			$f_1(x)$ (Hz)	$f_2(x)$ (mm)	$f_3(x)$ (mm)	$f_4(x)$ (MPa)	n	MPCI
Case 1	The current method	$T_2 = 0.45$ $L_2 = 27.5$ $T_3 = 0.78$ $L_3 = 18$	$R_p = 79.5179$ $R_s = 76.062$ $E = 4.54\%$	$R_p = 1.8977$ $R_s = 1.7611$ $E = 7.75\%$	$R_p = 0.0224$ $R_s = 0.0216$ $E = 3.70\%$	$R_p = 210.382$ $R_s = 223.38$ $E = 5.81\%$	$R_p = 2.390$ $R_s = 2.155$ $E = 1.09\%$	0.848
Case 2	The current method	$T_2 = 0.45$ $L_2 = 27.5$ $T_3 = 0.69$	$R_p = 76.7435$ $R_s = 74.205$ $E = 3.42\%$	$R_p = 1.8266$ $R_s = 1.8350$ $E = 0.45\%$	$R_p = 0.0211$ $R_s = 0.0214$ $E = 1.40\%$	$R_p = 236.027$ $R_s = 227.210$ $E = 3.88\%$	$R_p = 2.131$ $R_s = 2.213$ $E = 3.70\%$	0.640

It can infer that the proposed computational scheme is greater than TF. Besides, case 1 is adopted as an optimal candidate thanks to its highest MPCI value of 0.848.

Figures 10(a) and 10(b) illustrate the deformation and stress distributions of the mechanism, respectively.

4.4. Comparisons among Different Methods. The previous section shows that the computational method outperforms the TF in searching a global optimal solution of the 1-DOF mechanism. The comparison of the behaviors of the suggested method with other algorithms includes ANFIS-teaching-learning-based algorithm (ANFIS-coupled TLBO) [44] and ANFIS-Jaya [45]. Nonparameter statistical investigations are performed and involved in resolving case 1. In Table 15, the MPCI is almost the same for three methods. However, the output responses of the mechanism from the suggested method are better than those from the other algorithms.

Two nonparameter statistical techniques [57] are employed to determine the behaviors of three methods. Each method has 60 runs. As given in Table 16, it is inferred that the suggested computational method is superior to other methods.

In Table 17, the results of Friedman tests also prove that the computational method outperformed the others.

In order to compare the convergence speed among different algorithms in the literature, the proposed method (a hybridization of desirability, fuzzy, and ANFIS-based MFO) is compared with the ant lion optimizer (ALO) [48], particle swarm optimization-based gravitational search algorithm (PSOGSA) [49], and sine-cosine algorithm (SCA) [50]. A maximum iteration of 10000 and initial population of 20 are used for all algorithms. The results found that the current method in this study has faster convergence than others because the devoted method only needs a computation time of 559.78 s, as given in Table 18.

Additionally, the superiority of the current method in this paper is also compared with the Taguchi, the desirability, and Taguchi-fuzzy methods. It is remarked that the Taguchi method is able to search the optimal solution for each response (single optimization problem), while the others are used to solve the MOO problems for case study 1. Datasets in Table 7 are used for the Taguchi, Taguchi-fuzzy, and desirability methods. The results are summarized in Table 19.

From the results of Table 19, it can be revealed that, for optimization of a single response, the Taguchi method is a more suitable tool. By using the Taguchi, the optimal parameters are found with respect to each response but it only finds the optimum value for a single cost function, as shown in Table 19. By using the Taguchi-fuzzy method, the results searched the optimal sets of parameters for MOO but this approach is based on the Taguchi reasoning. This means that the optimal solutions can be also local values. Besides, using the desirability, the results found the optimal parameters for the MOO but this technique is based on the prediction precision of the mathematical models. Lastly, the current method (a hybridization of desirability, fuzzy, and ANFIS-based MFO methods) is a reliable technique that is superior to others because it can search the global solution for the 1-DOF mechanism.

Strengths of the proposed method's framework can be listed as follows:

(i) The behaviors of the 1-DOF mechanism are easily analyzed by linear/nonlinear FEM

(ii) Influence of the units of performances on the finally optimal solution can be ignored via the desirability method

(iii) The multiple design targets are easily converted into a single cost function through the FIS

(iv) The unknown relation among the design variables and the single cost function can be precisely approximated by ANFIS

(v) The global optimum solution of the 1-DOF mechanism can be achieved via the ANFIS-based MFO

However, this study still has drawbacks, including the computational principle and adaptive process. The computational principle requires a variety of different methods from statistics, numerical method, intelligent method, and metaheuristics. Besides, the adaptive process needs an adaptive update of new design variables and performances have not been studied yet. Finally, the computational methods have not been automatically connected.

At last, limitations of the present design framework concentrate on time and computational complexity as well as efficiency. This method needs a long period of computing time for each method. The computational complexity is mainly dependent on computer ability and experiences in the field. For a complex mechanism, the FEM and working time of computer are restricted.

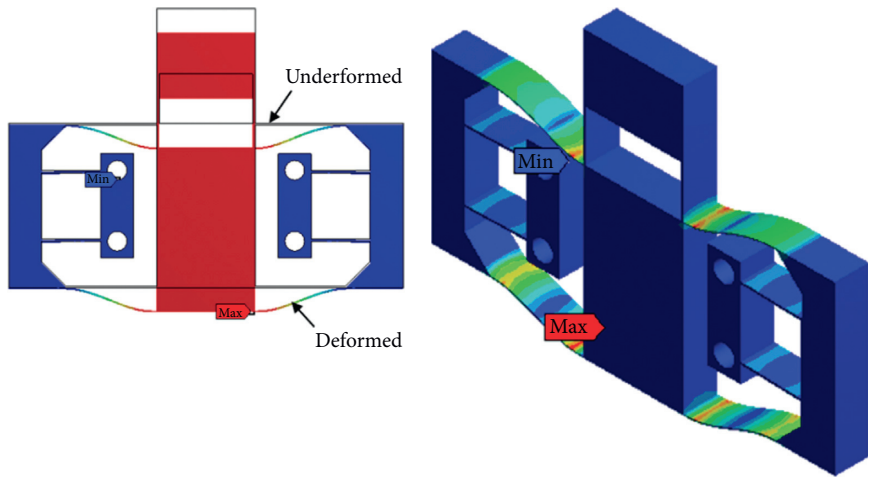

(a) (b)

Figure 10: Simulations for case 1: (a) deformation and (b) stress distribution.

Table 15: Comparison among different methods.

Approaches	$f_1(x)$ (Hz)	$f_2(x)$ (mm)	MPCI
ANFIS-Jaya ($T_2 = 0.45$ mm, $L_2 = 27.49$ mm, $T_3 = 0.77$ mm, $L_3 = 18$ mm)	76.880	1.719	0.848
ANFIS-TLBO ($T_2 = 0.45$ mm, $L_2 = 27.45$ mm, $T_3 = 0.78$ mm, $L_3 = 18$ mm)	76.376	1.746	0.848
The current method ($T_2 = 0.45$ mm, $L_2 = 27.5$ mm, $T_3 = 0.78$ mm, $L_3 = 18$ mm)	79.517	1.897	0.848

Table 16: Results of Wilcoxon tests.

Frequency		
	The current method and ANFIS-coupled Jaya	
Wilcoxon index	p value	Difference
0	≤0.001	−2.6379
	The current method and ANFIS-coupled TLBO	
Wilcoxon index	p value	Difference
0	≤0.001	−3.1419
Displacement		
	The current method and ANFIS-coupled Jaya	
Wilcoxon index	p value	Difference
0	≤0.001	−0.1786
	The current method versus ANFIS-coupled TLBO	
Wilcoxon index	p value	Difference
0	≤0.001	−0.1513

Table 17: Results of Friedman tests.

Frequency		
Method	Average	Rank
ANFIS-coupled Jaya	76.8800	60
ANFIS-coupled TLBO	76.3760	180
The current method	79.5179	120
Overall	77.5913	
p value	≤0.001	
Displacement		
Method	Average	Rank
ANFIS-coupled Jaya	1.71910	60
ANFIS-coupled TLBO	1.74640	180
The current method	1.89770	120
Overall	1.78773	
p value	≤0.001	

Table 18: Statistical results for comparison among metaheuristic methods.

Method	Results		Time (s)
	Frequency (Hz)	Displacement (mm)	
ANFIS-coupled PSOGSA	79.421	1.892	616.038
ANFIS-coupled SCA	79.426	1.895	599.544
ANFIS-coupled ALO	79.425	1.893	623.20
ANFIS-coupled LAPO	79.517	1.897	2707.75
The current method	79.517	1.897	559.78

Table 19: Comparison among the current method, Taguchi method, and Taguchi-fuzzy method.

Method		Optimal results			
Taguchi (single optimization)	Parameters (mm)	$T_2 = 0.65$ $L_2 = 22.5$ $T_3 = 0.78$ $L_3 = 18$	$T_2 = 0.45$ $L_2 = 27.5$ $T_3 = 0.54$ $L_3 = 22$	$T_2 = 0.65$ $L_2 = 22.5$ $T_3 = 0.78$ $L_3 = 18$	$T_2 = 0.65$ $L_2 = 22.5$ $T_3 = 0.66$ $L_3 = 20$
	Response	$f_1(\mathbf{x})$ (Hz)	$f_2(\mathbf{x})$ (mm)	$f_3(\mathbf{x})$ (mm)	$f_4(\mathbf{x})$ (MPa)
	Value	139.474	1.760	0.008	90.405
Taguchi-fuzzy (MOO)	Parameters (mm)	$T_2 = 0.45,\ L_2 = 27.5,\ T_3 = 0.54,\ L_3 = 20$			
	Response	$f_1(\mathbf{x})$ (Hz)	$f_2(\mathbf{x})$ (mm)	$f_3(\mathbf{x})$ (mm)	$f_4(\mathbf{x})$ (MPa)
	Value	75.871	1.776	0.019	212.114
Desirability (MOO)	Parameters (mm)	$T_2 = 0.65,\ L_2 = 22.5,\ T_3 = 0.54,\ L_3 = 21.27$			
	Response	$f_1(\mathbf{x})$ (Hz)	$f_2(\mathbf{x})$ (mm)	$f_3(\mathbf{x})$ (mm)	$f_4(\mathbf{x})$ (MPa)
	Value	106.841	0.930	0.011	120.090
The current method (MOO)	Parameters (mm)	$T_2 = 0.45,\ L_2 = 27.5,\ T_3 = 0.78,\ L_3 = 18$			
	Response	$f_1(\mathbf{x})$ (Hz)	$f_2(\mathbf{x})$ (mm)	$f_3(\mathbf{x})$ (mm)	$f_4(\mathbf{x})$ (MPa)
	Value	79.517	1.897	0.022	210.382

5. Conclusions

This paper proposed the computational method and its application in design optimization of compliant mechanisms. The 1-DOF compliant mechanism is used as the study object. The suggested method is a hybridization of statistics, FEM, artificial intelligence, and metaheuristics. The usefulness of the suggested method is tested through the numerical examples and statistical comparisons. An initial 3D model in FEM is designed, and the numerical datasets are retrieved by FEA. ANOVA is used to redetermine two fine spaces of parameters, so-called populations in MFO. Based on the refined datasets, the desirabilities of the frequency and displacement are brought into the FIS system where two objective functions become a single objective function through establishment of the fuzzy if-then rules. ANFIS is then established as predictor involving the refined parameters and the output of FIS. In order to reach a global optimization, MFO algorithm is utilized to deal with the output of FIS. The results found that the frequency is 79.517 Hz and displacement is 1.897 mm for the 1-DOF mechanism. The devoted method is better than the Taguchi, Taguchi-integrated fuzzy, and desirability methods because it can search a global solution.

In finding the global optimum solution, the suggested method is a better technique in comparison with the Taguchi, desirability, and Taguchi-integrated fuzzy methods. Besides, the devoted method outperforms the other metaheuristic algorithms such as TLBO and Jaya in terms of better performances. Also, the devoted method is superior to PSOGSA, SCA, ALO, and LAPO in terms of faster convergence.

In future work, experiments are carried out to verify the optimized results. The current method will be extended to optimization problems with multiple constraints. Besides, the proposed method will be also considered to apply for multi-DOF compliant mechanisms.

Data Availability

The data used to support the findings of this study are included within the article.

Conflicts of Interest

The authors declare that they have no conflicts of interest.

Acknowledgments

This research was funded by the Vietnam National Foundation for Science and Technology Development (NAFOSTED) under Grant no. 107.01–2019.14.

References

[1] D. N. Nguyen, T. Dao, N. Le Chau, and V. A. Dang, *Hybrid Approach of Finite Element Method , Kigring Metamodel, and Multiobjective Genetic Algorithm for Computational Optimization of a Flexure Elbow Joint for Upper-Limb Assistive*

Device, Springer, Berlin, Germany, 2019, https://www.springer.com/engineering/electronics/j.

[2] M. Ling, S. Chen, Q. Li, and G. Tian, "Dynamic stiffness matrix for free vibration analysis of flexure hinges based on non-uniform Timoshenko beam," *Journal of Sound and Vibration*, vol. 437, pp. 40–52, 2018.

[3] S.-C. Huang and T.-P. Dao, "Multi-objective optimal design of a 2-DOF flexure-based mechanism using hybrid approach of grey-taguchi coupled response surface methodology and entropy measurement," *Arabian Journal for Science and Engineering*, vol. 41, 2016.

[4] M. Ling, J. Cao, Z. Jiang, and Q. Li, "Development of a multistage compliant mechanism with new boundary constraint," *Review of Scientific Instruments*, vol. 89, 2018.

[5] R. K. Jain, S. Majumder, B. Ghosh, and S. Saha, "Design and manufacturing of mobile micro manipulation system with a compliant piezoelectric actuator based micro gripper," *Journal of Manufacturing Systems*, vol. 35, pp. 76–91, 2015.

[6] X. Zhou, H. Xu, J. Cheng, N. Zhao, and S. C. Chen, "Flexure-based Roll-to-roll Platform: a practical solution for realizing large-area microcontact printing," *Scientific Reports*, vol. 5, pp. 1–10, 2015.

[7] S. Polit and J. Dong, "Development of a high-bandwidth XY nanopositioning stage for high-rate micro-/nano-manufacturing," *Institute of Electrical and Electronics Engineers/American Society of Mechanical Engineers Transactions on Mechatronics*, vol. 16, no. 4, pp. 724–733, 2011.

[8] P. Wang and Q. Xu, "Design and modeling of constant-force mechanisms: a survey," *Mechanism and Machine Theory*, vol. 119, pp. 1–21, 2018.

[9] Y. S. Oh and S. Kota, "Synthesis of multistable equilibrium compliant mechanisms using combinations of bistable Mechanisms," *Journal of Mechanical Design*, vol. 131, pp. 0210021–02100211, 2009.

[10] S. Kota, J. Joo, Z. Li, S. M. Rodgers, and J. Sniegowski, "Design of compliant mechanisms: applications to MEMS, analog integr," *Analog Integrated Circuits and Signal Processing*, vol. 29, no. 1/2, pp. 7–15, 2001.

[11] S. Rakuff and J. F. Cuttino, "Design and testing of a long-range, precision fast tool servo system for diamond turning," *Precision Engineering*, vol. 33, no. 1, pp. 18–25, 2009.

[12] J. Granstrom, J. Feenstra, H. A. Sodano, and K. Farinholt, "Energy harvesting from a backpack instrumented with piezoelectric shoulder straps," *Smart Materials and Structures*, vol. 16, no. 5, pp. 1810–1820, 2007.

[13] J. J. Uicker, G. R. Pennock, J. E. Shigley, and J. M. McCarthy, "Theory of machines and mechanisms," *The Journal of Mechanical Design*, vol. 125, no. 3, p. 650, 2003.

[14] A. Midha, L. L. Howell, and T. W. Norton, "Limit positions of compliant mechanisms using the pseudo-rigid-body model concept," *Mechanism and Machine Theory*, vol. 35, no. 1, pp. 99–115, 2000.

[15] L. L. Howell, *Compliant Mechanisms*, John Wiley & Sons, Hoboken, NJ, USA, 2011.

[16] N. Lobontiu, *Nicolae Lobontiu-Compliant Mechanisms_ Design of Flexure Hinges*, CRC Press, Boca Raton, FL, USA, 2002.

[17] Y. Koseki, T. Tanikawa, N. Koyachi, and T. Arai, "Kinematic analysis of a translational 3-d.o.f. micro-parallel mechanism using the matrix method," *Advanced Robotics*, vol. 16, no. 3, pp. 251–264, 2002.

[18] M. Ling, J. Cao, Z. Jiang, and J. Lin, "Theoretical modeling of attenuated displacement amplification for multistage compliant mechanism and its application," *Sensors and Actuators A: Physical*, vol. 249, pp. 15–22, 2016.

[19] M. Ling, J. Cao, and N. Pehrson, "Kinetostatic and dynamic analyses of planar compliant mechanisms via a two-port dynamic stiffness model," *Precision Engineering*, vol. 57, pp. 149–161, 2019.

[20] S. T. Smith, D. G. Chetwynd, and D. K. Bowen, "Design and assessment of monolithic high precision translation mechanisms," *Journal of Physics E*, vol. 20, no. 8, pp. 977–983, 1987.

[21] S. Awtar and S. Sen, "A generalized constraint model for two-dimensional beam flexures: nonlinear load-displacement formulation," *Journal of Mechanical Design Transmission ASME*, vol. 132, pp. 0810081–08100811, 2010.

[22] Q. Xu and Y. Li, "Analytical modeling, optimization and testing of a compound bridge-type compliant displacement amplifier," *Mechanism and Machine Theory*, vol. 46, no. 2, pp. 183–200, 2011.

[23] W.-L. Zhu, Z. Zhu, P. Guo, and B.-F. Ju, "A novel hybrid actuation mechanism based XY nanopositioning stage with totally decoupled kinematics," *Mechanical Systems and Signal Processing*, vol. 99, pp. 747–759, 2018.

[24] B. Zhu, X. Zhang, and N. Wang, "Topology optimization of hinge-free compliant mechanisms with multiple outputs using level set method," *Structural and Multidisciplinary Optimization*, vol. 47, no. 5, pp. 659–672, 2013.

[25] Q. Chen, X. Zhang, H. Zhang, B. Zhu, and B. Chen, "Topology optimization of bistable mechanisms with maximized differences between switching forces in forward and backward direction," *Mechanism and Machine Theory*, vol. 139, pp. 131–143, 2019.

[26] N. Wang, Z. Zhang, X. Zhang, and C. Cui, "Optimization of a 2-DOF micro-positioning stage using corrugated flexure units," *Mechanism and Machine Theory*, vol. 121, pp. 683–696, 2018.

[27] M. Liu, X. Zhang, and S. Fatikow, "Design and analysis of a high-accuracy flexure hinge," *Review of Scientific Instruments*, vol. 87, 2016.

[28] T.-P. Dao and S.-C. Huang, "Design and multi-objective optimization for a broad self-amplified 2-DOF monolithic mechanism," *Sādhanā*, vol. 42, no. 9, pp. 1527–1542, 2017.

[29] K.-B. Choi and C. S. Han, "Optimal design of a compliant mechanism with circular notch flexure hinges," *Proceedings of the Institution of Mechanical Engineers, Part C: Journal of Mechanical Engineering Science*, vol. 221, no. 3, pp. 385–392, 2007.

[30] G. G. Fossati, L. F. F. Miguel, and W. J. P. Casas, "Multi-objective optimization of the suspension system parameters of a full vehicle model," *Optimization and Engineering*, vol. 20, no. 1, pp. 151–177, 2019.

[31] C. Butler, "A primer on the Taguchi method," *Computer Integrated Manufacturing Systems*, vol. 5, no. 3, p. 246, 1992.

[32] N. R. Costa, J. Lourenço, and Z. L. Pereira, "Desirability function approach: a review and performance evaluation in adverse conditions," *Chemometrics and Intelligent Laboratory Systems*, vol. 107, no. 2, pp. 234–244, 2011.

[33] S.-C. Huang and T.-P. Dao, "Multi-objective optimal design of a 2-DOF flexure-based mechanism using hybrid approach of grey-taguchi coupled response surface methodology and entropy measurement," *Arabian Journal for Science and Engineering*, vol. 41, no. 12, pp. 5215–5231, 2016.

[34] T.-P. Dao, "Multiresponse optimization of a compliant guiding mechanism using hybrid taguchi-grey based fuzzy logic approach," *Mathematical Problems in Engineering*, vol. 2016, Article ID 5386893, 17 pages, 2016.

[35] M. V. Arasu, S. Arokiyaraj, P. Viayaraghavan et al., "One step green synthesis of larvicidal, and azo dye degrading

antibacterial nanoparticles by response surface methodology," *Journal of Photochemistry and Photobiology B: Biology*, vol. 190, pp. 154–162, 2019.

[36] K. J. Kim and D. K. J. Lin, "Optimization of multiple responses considering both location and dispersion effects," *European Journal of Operational Research*, vol. 169, no. 1, pp. 133–145, 2006.

[37] P. Jiang, C. Wang, Q. Zhou, X. Shao, L. Shu, and X. Li, "Optimization of laser welding process parameters of stainless steel 316L using FEM, Kriging and NSGA-II," *Advances in Engineering Software*, vol. 99, pp. 147–160, 2016.

[38] D. Singh, V. Kumar, Vaishali, and M. Kaur, "Classification of COVID-19 patients from chest CT images using multi-objective differential evolution–based convolutional neural networks," *European Journal of Clinical Microbiology & Infectious Diseases*, vol. 39, no. 7, pp. 1379–1389, 2020.

[39] R. Rathi, C. Prakash, S. Singh, G. Krolczyk, and C. I. Pruncu, "Measurement and analysis of wind energy potential using fuzzy based hybrid madm approach," *Energy Reports*, vol. 6, pp. 228–237, 2020.

[40] H. S. Pannu, D. Singh, and A. K. Malhi, "Multi-objective particle swarm optimization-based adaptive neuro-fuzzy inference system for benzene monitoring," *Neural Computing and Applications*, vol. 31, no. 7, pp. 2195–2205, 2019.

[41] M. Keshtiara, S. Golabi, and R. Tarkesh Esfahani, "Multi-objective optimization of stainless steel 304 tube laser forming process using GA," *Engineering Computations*, vol. 37, 2019.

[42] S. Chatterjee, S. Sarkar, S. Hore, N. Dey, A. S. Ashour, and V. E. Balas, "Particle swarm optimization trained neural network for structural failure prediction of multistoried RC buildings," *Neural Computing and Applications*, vol. 28, pp. 2005–2016, 2017.

[43] T.-P. Dao, S.-C. Huang, and P. T. Thang, "Hybrid Taguchi-cuckoo search algorithm for optimization of a compliant focus positioning platform," *Applied Soft Computing-Journal*, vol. 57, 2017.

[44] R. V. Rao, V. J. Savsani, and D. P. Vakharia, "Teaching-learning-based optimization: a novel method for constrained mechanical design optimization problems," *Computer-Aided Design*, vol. 43, no. 3, pp. 303–315, 2011.

[45] R. V. Rao, H. S. Keesari, P. Oclon, and J. Taler, "An adaptive multi-team perturbation-guiding Jaya algorithm for optimization and its applications," *Engineering Computations*, vol. 36, no. 1, pp. 391–419, 2019.

[46] A. F. Nematollahi, A. Rahiminejad, and B. Vahidi, "A novel physical based meta-heuristic optimization method known as Lightning Attachment Procedure Optimization," *Applied Soft Computing*, vol. 59, pp. 596–621, 2017.

[47] S. Mirjalili, "Moth-flame optimization algorithm: a novel nature-inspired heuristic paradigm," *Knowledge-Based System*, vol. 89, pp. 228–249, 2015.

[48] S. Mirjalili, "The ant lion optimizer," *Advances in Engineering Software*, vol. 83, 2015.

[49] S. Mirjalili and S. Z. M. Hashim, "A new hybrid PSOGSA algorithm for function optimization," in *Proceedings ICCIA 2010-2010 International Conference on Computer and Information Application*, Tianjin, China, July 2010.

[50] S. Mirjalili, "SCA: A sine cosine algorithm for solving optimization problems," *Knowledge-Based System*, vol. 96, 2016.

[51] M. A. Díaz-Cortés, E. Cuevas, J. Gálvez, and O. Camarena, "A new metaheuristic optimization methodology based on fuzzy logic," *Applied Soft Computing*, vol. 61, pp. 549–569, 2017.

[52] N. Le Chau, N. T. Tran, and T. P. Dao, "A multi-response optimal design of bistable compliant mechanism using efficient approach of desirability, fuzzy logic, ANFIS and LAPO algorithm," *Applied Soft Computing-Journal*, vol. 94, 2020.

[53] J. Zhou, C. Li, C. A. Arslan, M. Hasanipanah, and H. Bakhshandeh Amnieh, "Performance evaluation of hybrid FFA-ANFIS and GA-ANFIS models to predict particle size distribution of a muck-pile after blasting," *Engineering Computations*, vol. 37, 2019.

[54] Q. Liu, X. Zhou, P. Xu, Q. Zou, and C. Lin, "A flexure-Based long-Stroke fast tool servo for diamond turning," *The International Journal of Advanced Manufacturing Technology*, vol. 59, 2012.

[55] Z. Zhu, X. Zhou, Q. Liu, and S. Zhao, "Multi-objective optimum design of fast tool servo based on improved differential evolution algorithm," *Journal of Mechanical Science and Technology*, 2011.

[56] W. Le Zhu, X. Yang, F. Duan, Z. Zhu, and B. F. Ju, "Design and adaptive terminal sliding mode control of a fast tool servo system for diamond machining of freeform surfaces," *Institute of Electrical and Electronics Engineers Transactions on Industrial Electronics*, 2019.

[57] S. García, D. Molina, M. Lozano, and F. Herrera, "A study on the use of non-parametric tests for analyzing the evolutionary algorithms' behaviour: a case study on the CEC'2005 Special Session on Real Parameter Optimization," *Journal of Heuristics*, vol. 15, no. 6, pp. 617–644, 2009.